Author/s:
Lin, G;Richardson, JJ;Ahmed, H;Besford, QA;Christofferson, AJ;Beyer, S;Lin, Z;Rezk, AR;Savioli, M;Zhou, J;McConville, CF;Cortez-Jugo, C;Yeo, LY;Caruso, F

Title:
Programmable Phototaxis of Metal–Phenolic Particle Microswimmers

Date:
2021-04-01

Citation:
Lin, G., Richardson, J. J., Ahmed, H., Besford, Q. A., Christofferson, A. J., Beyer, S., Lin, Z., Rezk, A. R., Savioli, M., Zhou, J., McConville, C. F., Cortez-Jugo, C., Yeo, L. Y. & Caruso, F. (2021). Programmable Phototaxis of Metal–Phenolic Particle Microswimmers. Advanced Materials, 33 (13), https://doi.org/10.1002/adma.202006177.

Programmable Phototaxis of Metal–Phenolic Particle Microswimmers

*Gan Lin, Joseph J. Richardson, Heba Ahmed, Quinn A. Besford, Andrew J. Christofferson, Sebastian Beyer, Zhixing Lin, Amgad R. Rezk, Marco Savioli, Jiajing Zhou, Chris F. McConville, Christina Cortez-Jugo, Leslie Y. Yeo, and Frank Caruso**

Dr. G. Lin, Dr. J. J. Richardson, Dr. Q. A. Besford,[+] Z. Lin, M. Savioli,[++] Dr. Jiajing Zhou, Dr. C. Cortez-Jugo, Prof. F. Caruso
ARC Centre of Excellence in Convergent Bio-Nano Science and Technology, and the Department of Chemical Engineering, The University of Melbourne, Parkville, Victoria 3010, Australia
E-mail: fcaruso@unimelb.edu.au

Dr. H. Ahmed, Dr. A. R. Rezk, Prof. L. Y. Yeo
Micro/Nanophysics Research Laboratory, School of Engineering, RMIT University, Melbourne, Victoria 3000, Australia

Dr. A. J. Christofferson, Prof. C. F. McConville
School of Science, College of Science, Engineering and Health, RMIT University, Melbourne, Victoria 3001, Australia

Dr. S. Beyer
Department of Biomedical Engineering, The Chinese University of Hong Kong, Shatin, Hong Kong, China

[+]Present address: Leibniz Institute for Polymer Research, 01069 Dresden, Germany
[++]Present address: Department of Chemical Science and Technology, University of Rome Tor Vergata, Via della Ricerca Scientifica 1, 00133 Rome, Italy

Keywords: light-driven, micromotors, cargo loading, tunable speed, spectral response

Light-driven directional motion is common in nature but remains a challenge for synthetic microparticles, particularly regarding collective motion on a macroscopic scale. Successfully engineering microparticles with light-driven collective motion could lead to breakthroughs in drug delivery, contaminant sensing, environmental remediation, and artificial life. Herein, metal–phenolic particle microswimmers capable of autonomously sensing and swimming toward an external light source are reported, with the speed regulated by the wavelength and intensity of illumination. These microswimmers can travel macroscopic distances (centimeters) and can remain illuminated for hours without degradation of motility. Experimental and theoretical analyses demonstrate that motion is generated through chemical transformations of the organic component of the metal–phenolic complex. Furthermore, cargo

with specific spectral absorption profiles can be loaded into the particles and endow the particle microswimmers with activated motion corresponding to these spectral characteristics. The programmable nature of the light navigation, tunable size of the particles, and versatility of cargo loading demonstrate the versatility of these metal–phenolic particle microswimmers.

Phototaxis, the directional motion toward or away from light, is a natural phenomenon that has inspired the construction of synthetic light-steered particle microswimmers, using different mechanisms for motility including catalysis, photothermal effects, and molecular conformational transformation[1–6] for applications such as remediation[7] and drug delivery.[8] Still, precise control over both direction and speed is challenging, especially across large length scales (e.g., centimeter scale).[9,10] Herein, we use Zn^{2+} and ellagic acid to design metal–phenolic particle microswimmers capable of autonomously sensing and swimming toward an external light source (positive phototaxis) at both microscopic and macroscopic scales. The speed of motion is regulated by the solvent and the wavelength and intensity of illumination. Furthermore, the incorporation of cargo allows for multi-wavelength actuation. The experimental and theoretical analyses demonstrate that motion is generated through conformational transformation of the phenolic ligands upon illumination, which generates a large twist in the planar molecule to propel the particles forward. The complex and responsive nature of motility demonstrated in this work advances research in the development of adaptive autonomous microsystems.[11,12]

Metal–phenolic materials have recently received interest owing to their versatile coordination chemistry[13] and promise in various environmental and biological applications.[14] The metal–phenolic particle microswimmers synthesized in the present work were obtained by mixing the phenolic ligand ellagic acid (EA) with zinc acetate in *N*-methyl-2-pyrrolidone (NMP) solution, triggering the coordination-driven self-assembly of porous crystalline particles with a high yield (~90% by mass) (**Figure 1**). The successful

coordination between EA and zinc ions (Zn^{2+}) was confirmed by the elemental composition of the particles and disappearance of characteristic O–H vibration peaks (~3144 cm^{-1}) in the Fourier transform infrared spectrum of the particle microswimmers (Figure S1 and S2). The diameter of the particle microswimmers was tuned from 1 to 4 μm by adjusting the concentration of the starting precursors (Figure S3). Hereafter, particle microswimmers with uniform dispersity and a diameter of 3 μm (Figure 1c, d) are discussed. Powder X-ray diffraction (XRD) patterns showed that the particle microswimmers were crystalline, with a distinct crystallinity from that of the two precursors (Figure 1e). Similar to many other crystalline metal–organic materials,[15] the particle microswimmers were porous—nitrogen adsorption analysis revealed a bimodal hierarchical nanopore architecture with pore sizes of ~8 and ~12 nm and a surface area of 33.1 m^2 g^{-1} (Figure S4).

Controlling the velocity, that is both the direction and speed, has been sought after in micromotor research as this allows for a wider variety of potential applications.[16] Stimuli other than light, such as magnetic fields and chemical gradients, are often used to control the velocity of microswimmers for various applications; however, light has the potential to offer numerous avenues for tuning the velocity of microswimmers (e.g., intensity, wavelength, direction).[17,18] The particle microswimmers displayed positive phototaxis under ultraviolet (UV) light at both the microscopic and macroscopic scales in NMP. Movement of the particle microswimmers toward UV light was apparent with the naked eye (macroscopic scale) (**Figure 2**a). As observed under the microscope, exposure of the particle microswimmers (dispersed in NMP) to UV light (~365 nm) caused the particle microswimmers to move toward the focal point of illumination (Figure 2b, c and Movie S1). In contrast, exposure to white (broad spectrum), blue (~470 nm), green (~535 nm), or orange (~620 nm) light failed to induce a response in the particle microswimmers (Figure 2d, Figure S5, Movie S2). Furthermore, the autonomous directional motion of the particle microswimmers could be repeatedly activated and deactivated by turning the light on and off, respectively, without any

reduction in speed across subsequent "on" and "off" steps (Figure 2e, Movie S3). The movement speed of the particle microswimmers increased linearly up to 102 μm s^{-1} as the light intensity increased to 0.60 mW cm^{-2} (Figure 2f, Figure S6). Photothermal effects were ruled out as the temperature of the suspension did not increase over time (Figure S7), and photothermal micromotors typically move away from light, rather than toward light.[3,19]

Advanced self-propelled systems have been developed based on the photoreactions of organic molecules, which thereby induce mechanical motion, including walking, bending, rotation, and organization.[6,20–22] To gain a further understanding of the phototaxis of the particle microswimmers, the experiments were performed in five different solvents of varying polarities, that is water, 1-butanol, dimethyl sulfoxide (DMSO), dimethylformamide (DMF), and 1,4-dioxane (Movie S4). The results showed that the motion and speed of the particle microswimmers was dependent on the polarity of the solvent (Table S1, Figure S8 and S9), which suggests that the positive phototaxis is likely driven by the conformational transformation of EA at the molecular level when exposed to UV illumination. Specifically, the speed correlated inversely with the polarity of the solvent, whereas no distinct correlation was observed with the viscosity and refractive index of the solvent or the fluorescence of the particle microswimmers (Table S1).

Quantum mechanics (QM) calculations in DMF were performed to identify the possible chemical reaction pathways of free EA under UV light. The findings as illustrated in **Figure 3**a revealed the occurrence of a transition in EA upon exposure to UV illumination at ~365 nm, resulting in an excited-state structure with a single proton transferred from the adjacent hydroxyl group to the ether oxygen. In the photo-induced proton transfer intermediate structure, the distance between the remaining ether oxygen and the adjacent hydroxyl proton is reduced by 0.15 Å relative to that in the initial structure (Figure S10). This conformation affords a possible non-radiative structural relaxation pathway, where a second proton transfer occurs coupled with a twist (~55°) in the structure as a short-lived double ketene is formed,

producing rapid and reversible twisting. The dark side of the particle microswimmers (side farthest from the light source) has a higher likelihood to fully relax and can therefore undergo more propulsive transformations. Altogether, these pathways lead to movement of the particle microswimmers toward UV light.

The effect of the EA transition pathway on motion was further elucidated by performing the same calculations in the other four different solvents (Table S2). For the aprotic solvents (DMSO, DMF, and 1,4-dioxane), the transformation pathway, which involves a photo-induced proton transfer and a second proton transfer relaxation pathway, required less energy than that in the polar protic solvents (water and 1-butanol). Moreover, in the aprotic solvents there was a large (~55°) twist in the resulting chemical structure after transition as opposed to the slight-to-no twist and higher-energy products observed in the protic solvents. This analysis confirmed the experimental results, which showed that the light-induced movement is more favorable in low polarity solvents (Table S1). Collectively, these results demonstrate that the chemical environment, which determines the threshold energy for proton transfer and subsequent molecular twist to occur, offers an additional route for modulating the motility of the particle microswimmers.

Under prolonged UV light illumination (e.g., >12 h), the micromotors eventually lost motility as seen under the microscope (Figure S11, Movie S5). This loss of movement, along with the reduced mobility and impaired molecular twist in protic solvents, suggested that the presence of trace water could react with EA to form hexahydroxydiphenic acid (HHDP).[23] Therefore, ^{1}H NMR spectroscopy was used to examine molecular changes in free EA before and after UV illumination. After UV illumination, two new peaks (11.34 and 11.86 ppm) emerged in the EA spectrum. The former peak was assigned to the newly formed hydroxyl group and the latter peak to the carbonyl group attached to the benzene group (Figure 3b, Table S3), confirming the formation of HHDP. The ratio between the areas of the peak corresponding to the hydroxyl group (11.34 ppm) and the peak corresponding to the proton

attached to the benzene ring (7.45 ppm) increased steadily to 1 with increasing illumination time (Figure 3c), suggesting gradual transformation of EA to HHDP. Owing to limitations in performing ^{1}H NMR studies on microparticles, Fourier transformed extended X-ray absorption fine structure (EXAFS) and Raman spectroscopy were used to investigate changes in the molecular structure at the atomic level and chemical structure of EA in the particle microswimmers. The Fourier transformed EXAFS spectra demonstrated a slight rearrangement in the position of scattering atoms adjacent to the zinc metal center the in the metal–phenolic (EA-Zn) particle microswimmers after 12 h of UV illumination (Figure 3d). This was likely due to the chemical change of EA after illumination, leading to an increased distance between the Zn atom and its nearest neighbors, which indicates the occurrence of conformational changes. The Raman spectra showed that the intensity of the peak corresponding to the benzene ring stretching (1580 cm^{-1}) increased gradually with increasing UV exposure time, whereas the C=O stretching peak (1700 cm^{-1}) remained largely unchanged (Figure 3e). The ratio between the intensities of these two peaks increased steadily with increasing exposure times up to 6 h, after which a plateau was reached (Figure S12). Collectively, these results support the QM predictions of light-induced conformational changes of the phenolic ligand and demonstrate that the particle microswimmers eventually lose their ability to move upon permanent transition of EA to HHDP.

To determine the broad applications of the particle micoswimmers, we examined the transport of cargo in the particle microswimmers in response to different light wavelengths. Specifically, the pores of the particle swimmers were loaded with aromatic cargo via interactions with the accessible metal binding sites and aromatic rings of EA likely through π–π stacking and/or metal–organic interactions. Three different commonly used functional molecules, i.e., juglone (Jug), doxorubicin (Dox), and rhodamine b (RhB) were chosen as cargo molecules (**Figure 4**a and Figure S13). Successful post-loading via incubation was confirmed by color changes of the particle microswimmers (Figure 4c). The loading

efficiencies varied between 15 and 99% depending on the cargo molecule and loading concentration, and the final content of the cargo varied between 1 and 12% (Table S4, Figure S14). Importantly, the loaded cargo did not compromise the motion of the particle microswimmers under UV illumination (Figure 4d, e, Figure S15–S17, Movie S6–S8).

Controlling micromotors with different wavelengths of light is important for the completion of complex tasks that require different subsets of micromotors to perform different roles in the same media.[24] As Jug, Dox, and RhB have distinct absorption properties (Figure S18), the absorption of different wavelengths of light by the cargo and related energy transfer to the particle microswimmers enabled modulation of the speed of the particle microswimmers toward the light. Raman spectroscopy with Jug as model cargo demonstrated a strong shift in the –OH vibration (from 1374 to 1337 cm^{-1}) after loading, indicating metal–organic coordinative interactions between Jug and Zn (Figure S19). Similar coordinative interactions could occur for Dox and RhB owing to their metal chelation sites (e.g., carbonyl groups and hydroxyl groups). The coordinative bond with Zn provides connected electrons, which likely enables energy transfer from aromatic cargo to EA during excitation. The non-loaded particle microswimmers exhibited positive phototaxis only upon exposure to UV light, whereas the cargo-loaded particle microswimmers selectively moved toward light with specific wavelengths corresponding to the absorption peaks of the cargo. Moreover, the broad absorption of Dox and RhB enabled the cargo-loaded particle microswimmers to display positive phototaxis under multiple channels of light (blue, green, and orange), with the speed regulated by the illumination wavelength and the light absorption properties of the cargo (Figure 4f, Figure S15–S17, Movie S6–S8). The results demonstrate that the metal–phenolic particle microswimmers are readily post-modified for distinct spectral responses simply by selecting the appropriate cargo. This flexibility has the potential to allow for the generation of different “species” of microswimmers each capable of moving toward different combinations of light wavelengths. To demonstrate their potential use in biomedical applications, the native

metal–phenolic microswimmers and Dox-loaded microswimmers were incubated with HeLa cells for 48 h. Notably, the native metal–phenolic microswimmers showed negligible cytotoxicity (Figure S20), suggesting good biocompatibility. In contrast, the Dox-loaded microswimmers exhibited enhanced cancer cell killing capability, comparable with free Dox, demonstrating the potential of the microswimmers for drug delivery.

We have presented a synthetic metal–phenolic particle microswimmer with rapid and sustained positive phototaxis. Our experimental and computational calculations provide insights into the mechanism behind the light-induced motion of these particle microswimmers. The metal–phenolic particle microswimmers present several advantages, including: i) simple and robust synthesis; ii) highly controlled direction and speed of movement (i.e., velocity) owing to the spatial and temporal precision of light;[25] iii) versatile cargo loading into the particle pores; and iv) programmable spectral response via cargo encapsulation. This work introduces a highly controllable particle microswimmer with promise for diverse applications in fields including robotics,[11] drug delivery,[8] and environmental applications.[7]

Supporting Information
Supporting Information is available from the Wiley Online Library or from the author.

Acknowledgements
This research was conducted and funded by the Australian Research Council Centre of Excellence in Convergent Bio-Nano Science and Technology (project number CE140100036). F.C. acknowledges the award of a National Health and Medical Research Council Senior Principal Research Fellowship (GNT1135806). This work was performed in part at the Materials Characterisation and Fabrication Platform (MCFP) at The University of Melbourne and the Victorian Node of the Australian National Fabrication Facility (ANFF). This research was undertaken with the assistance of resources and services (resource grant nr3) from the National Computational Infrastructure (NCI), which is supported by the Australian Government. We acknowledge Dr Ana Buzanich for assistance with EXAFS measurements and the Bessy II synchrotron. We thank Prof. Trevor Smith, Dr Christopher Hall, and Paul Brannon from The University of Melbourne for their assistance with microscopy experiments, Min Liu from The University of Melbourne for assistance with nitrogen adsorption analysis, and Dr Sukhvir Kaur Bhangu and Dr René Lafleur from The University of Melbourne for discussion on NMR.

Conflicts of Interest
The authors declare no competing interests.

Data Availability Statement
The data that support the findings of this study are available from the corresponding author upon reasonable request.

Received: ((will be filled in by the editorial staff))
Revised: ((will be filled in by the editorial staff))
Published online: ((will be filled in by the editorial staff))

References

[1] B. Dai, J. Wang, Z. Xiong, X. Zhan, W. Dai, C.-C. Li, S.-P. Feng, J. Tang, *Nat. Nanotechnol.* **2016**, *11*, 1087.

[2] Y. Tu, F. Peng, D. A. Wilson, *Adv. Mater.* **2017**, *29*, 1701970.

[3] M. Xuan, Z. Wu, J. Shao, L. Dai, T. Si, Q. He, *J. Am. Chem. Soc.* **2016**, *138*, 6492.

[4] C. Chen, F. Mou, L. Xu, S. Wang, J. Guan, Z. Feng, Q. Wang, L. Kong, W. Li, J. Wang, Q. Zhang, *Adv. Mater.* **2017**, *29*, 1603374.

[5] L. Xu, F. Mou, H. Gong, M. Luo, J. Guan, *Chem. Soc. Rev.* **2017**, *46*, 6905.

[6] E. Uchida, R. Azumi, Y. Norikane, *Nat. Commun.* **2015**, *6*, 7310.

[7] B. Esteban-Fernández de Ávila, P. Angsantikul, D. E. Ramírez-Herrera, F. Soto, H. Teymourian, D. Dehaini, Y. Chen, L. Zhang, J. Wang, *Sci. Rob.* **2018**, *3*, eaat0485.

[8] X. Lin, Z. Wu, Y. Wu, M. Xuan, Q. He, *Adv. Mater.* **2016**, *28*, 1060.

[9] Y. Tu, F. Peng, X. Sui, Y. Men, P. B. White, J. C. M. van Hest, D. A. Wilson, *Nat. Chem.* **2017**, *9*, 480.

[10] Z. Guo, T. Wang, A. Rawa, J. Hou, Z. Cao, H. Zhang, J. Xu, Z. Gu, V. Chen, K. Liang, *Mater. Today* **2019**, *28*, 10.

[11] C. W. Shields, O. D. Velev, *Chem* **2017**, *3*, 539.

[12] J. Li, B. E.-F. de Ávila, W. Gao, L. Zhang, J. Wang, *Sci. Rob.* **2017**, *2*, eaam6431.

[13] H. Ejima, J. J. Richardson, K. Liang, J. P. Best, M. P. van Koeverden, G. K. Such, J. Cui, F. Caruso, *Science* **2013**, *341*, 154.

[14] M. A. Rahim, S. L. Kristufek, S. Pan, J. J. Richardson, F. Caruso, *Angew. Chem. Int. Ed.* **2019**, *58*, 1904.

[15] T. R. Cook, Y.-R. Zheng, P. J. Stang, *Chem. Rev.* **2013**, *113*, 734.

[16] L. Ricotti, B. Trimmer, A. W. Feinberg, R. Raman, K. K. Parker, R. Bashir, M. Sitti, S. Martel, P. Dario, A. Menciassi, *Sci. Rob.* **2017**, *2*, eaaq0495.

[17] M. You, C. Chen, L. Xu, F. Mou, J. Guan, *Acc. Chem. Res.* **2018**, *51*, 3006.

[18] K. Bente, A. Codutti, F. Bachmann, D. Faivre, *Small* **2018**, *14*, 1704374.

[19] D. Okawa, S. J. Pastine, A. Zettl, J. M. J. Fréchet, *J. Am. Chem. Soc.* **2009**, *131*, 5396.

[20] A. H. Gelebart, D. Jan Mulder, M. Varga, A. Konya, G. Vantomme, E. W. Meijer, R. L. B. Selinger, D. J. Broer, *Nature* **2017**, *546*, 632.

[21] H. Zhao, S. Sen, T. Udayabhaskararao, M. Sawczyk, K. Kučanda, D. Manna, P. K. Kundu, J.-W. Lee, P. Král, R. Klajn, *Nat. Nanotechnol.* **2016**, *11*, 82.

[22] K. Ichimura, S.-K. Oh, M. Nakagawa, *Science* **2000**, *288*, 1624.

[23] A. F. Aguilera-Carbo, C. Augur, L. A. Prado-Barragan, C. N. Aguilar, E. Favela-Torres, *Chem. Pap.* **2008**, *62*, 440.

[24] J. Zheng, B. Dai, J. Wang, Z. Xiong, Y. Yang, J. Liu, X. Zhan, Z. Wan, J. Tang, *Nat. Commun.* **2017**, *8*, 1438.

[25] T. van Leeuwen, A. S. Lubbe, P. Štacko, S. J. Wezenberg, B. L. Feringa, *Nat. Rev. Chem.* **2017**, *1*, 0096.

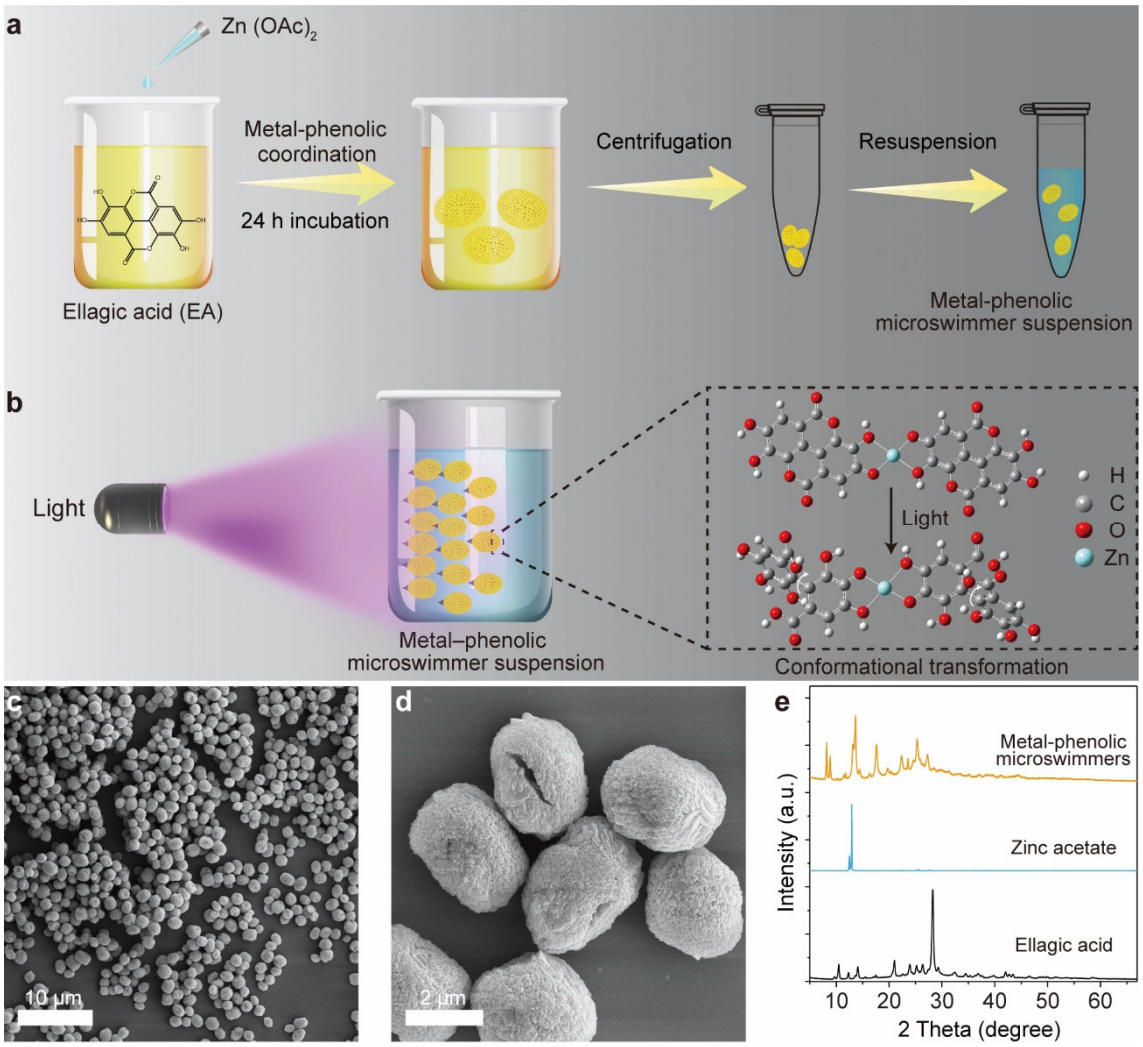

Figure 1. Preparation and characterization of metal–phenolic particle microswimmers. (a) Schematic illustration of the synthesis of the particle microswimmers. (b) Schematic illustration of the light-induced motion of the metal–phenolic microswimmers. (c, d) Scanning electron microscopy images of the particle microswimmers at low and high magnification, respectively. (e) XRD patterns of the metal–phenolic particle microswimmers, zinc acetate, and EA.

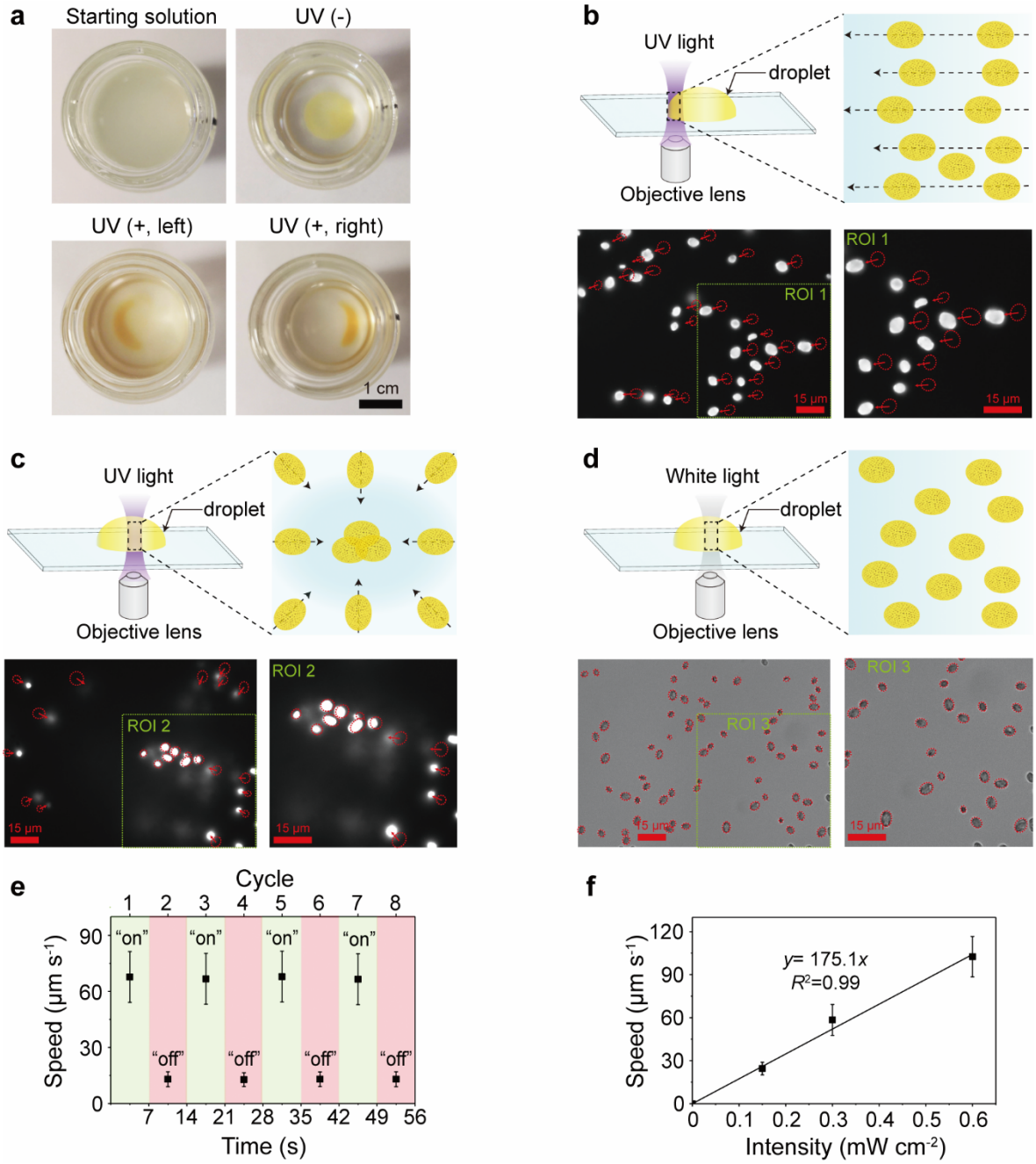

Figure 2. Light-steered positive phototaxis of metal–phenolic particle microswimmers. (a) Photographs showing vials containing the particle microswimmers before and after incubation under ambient conditions (no UV exposure, UV (−)) or UV light from the left side (UV (+, left)) or right side (UV (+, right)) of the vials for 9 h. The scale bar for all photographs is 1 cm. (b, c) Schematic illustrations and representative microscopy images showing the motion of the particle microswimmers near the edge (b) and at the centre (c) of an NMP droplet containing the particle microswimmers under UV illumination (~365 nm). (d) Schematic illustration and representative microscopy images of the metal–phenolic particle microswimmers in an NMP droplet exposed to white light. In (b)–(d), the red circles represent the initial positions of the particle microswimmers and the arrows indicate the direction of motion. The microscopy images were captured at 0.1 s after exposure to UV (or white) light. ROI, region of interest. (e) Speed of the particle microswimmers under "on"/"off" cycling of UV light (light intensity: 0.30 mW cm^{-2}). Note that roughly 1 min was required for convection to stop within the droplet and therefore the "off" speed is non-zero during rapid

cycling. (f) Variations in the speed of the particle microswimmers (near the edge of the droplet) as a function of UV light intensity. In (e) and (f), the values are the average speeds of at least 50 particles at three randomly selected time points, the error bars represent the standard deviations.

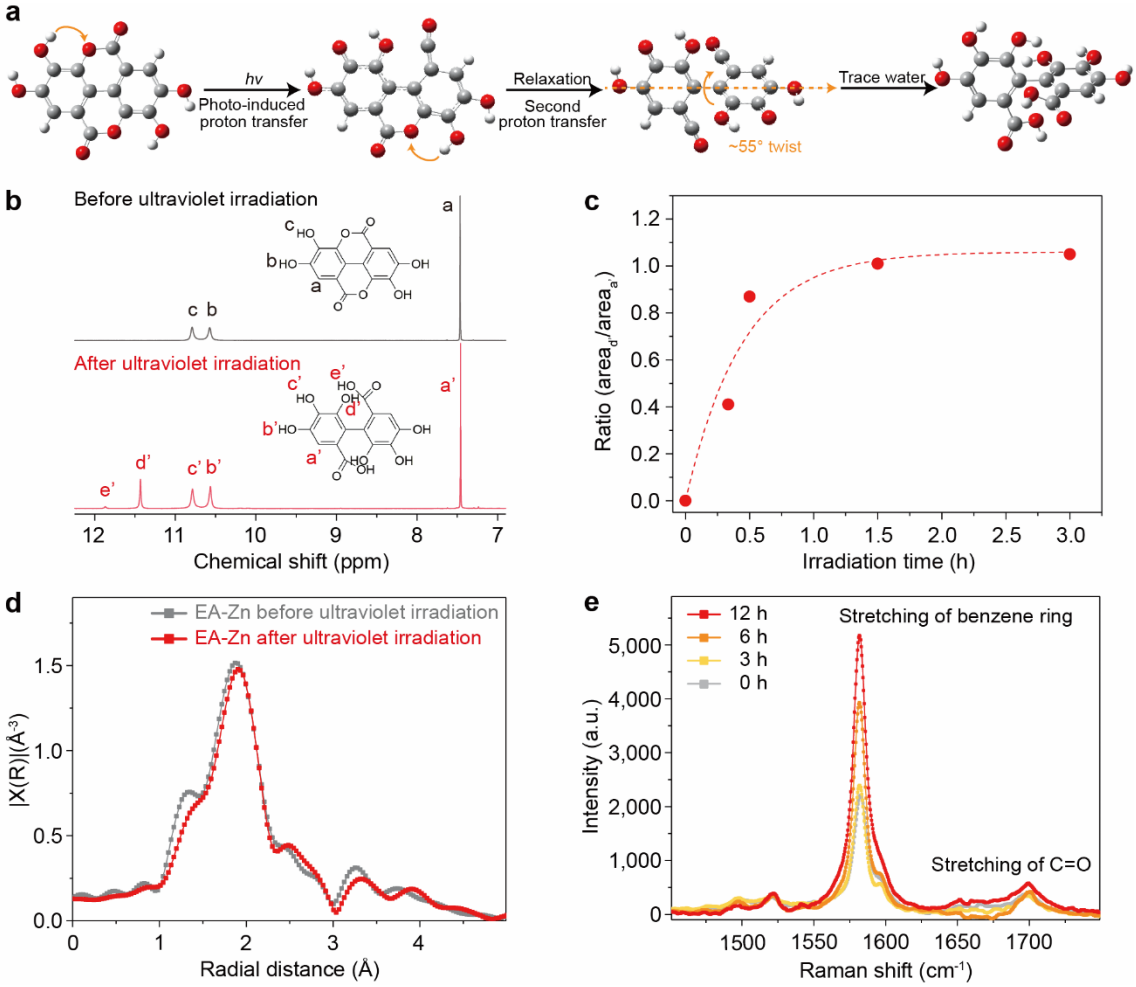

Figure 3. Theoretical and experimental analyses of the mechanism of light-steered motion for the metal–phenolic particle microswimmers. (a) Possible chemical pathway for the transformation of EA under UV illumination; the excited state was approximated by QM calculations in density functional theory. (b) ^{1}H-NMR spectra of EA before and after UV exposure for 0.5 h. (c) Ratio between the areas of the peak d′ at 11.34 ppm and peak a′ at 7.45 ppm over irradiation time using ^{1}H-NMR spectroscopy. (d) Fourier transformed EXAFS spectra of the particle microswimmers before and after UV illumination for 12 h. (e) Raman spectra of the particle microswimmers after UV illumination for 0, 3, 6, and 12 h.

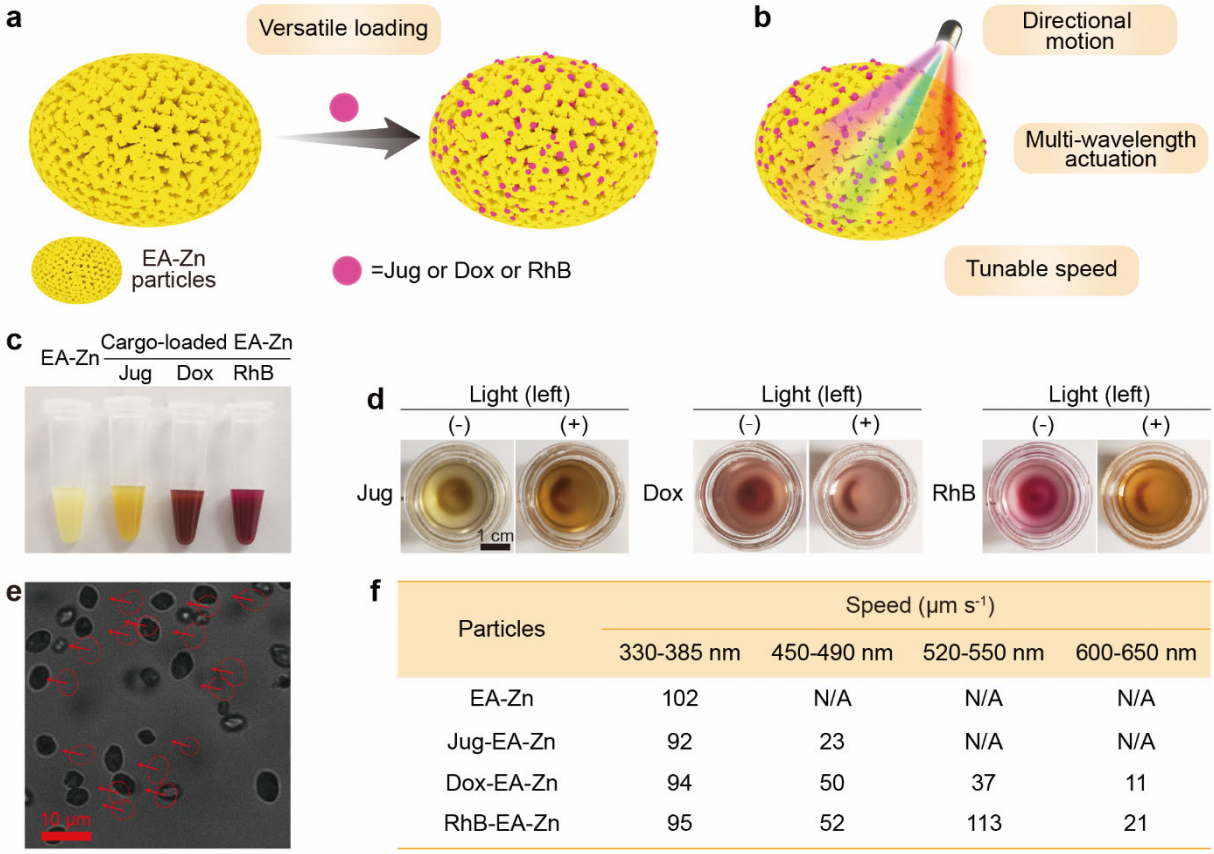

Particles	Speed (μm s^{-1})			
	330-385 nm	450-490 nm	520-550 nm	600-650 nm
EA-Zn	102	N/A	N/A	N/A
Jug-EA-Zn	92	23	N/A	N/A
Dox-EA-Zn	94	50	37	11
RhB-EA-Zn	95	52	113	21

Figure 4. Metal–phenolic particle microswimmers for versatile cargo loading and light-steered motion under different light wavelengths. (a) Schematic showing the encapsulation of different cargo, Jug, Dox, or RhB, in the particle microswimmers. (b) Features of the cargo-loaded particles as microswimmers. (c) Photograph of the particle microswimmers before and after loading with different cargos. (d) Photographs showing vials containing the cargo-loaded particle microswimmers subjected to no UV illumination (−) or UV illumination (+) from the left side of the vials. The scale bar for all photographs is 1 cm. (e) Microscopy image showing the motion of Dox-loaded particle microswimmers at the edge of an NMP droplet upon UV light exposure (0.60 mW cm^{-2}); the red circles represent the initial positions of the particles (before UV illumination) and the arrows represent the direction of motion of the particles. (f) Speeds of non-loaded (EA-Zn) and Jug-, Dox-, or RhB-loaded metal–phenolic particle microswimmers under different light wavelengths. N/A, not applicable.

Metal–organic microswimmers with precise light-driven velocities have been engineered with promise for robotics, drug delivery, and environmental applications. Various cargo with distinct spectral absorption profiles can be loaded into the microswimmers to tune the specific wavelengths of light that lead to motion under ultraviolet, blue, green, and orange light.

G. Lin, J. J. Richardson, H. Ahmed, Q. A. Besford, A. J. Christofferson, S. Beyer, Z. Lin, A. R. Rezk, M. Savioli, J. Zhou, C. F. McConville, C. Cortez-Jugo, L. Y. Yeo, F. Caruso*

Programmable Phototaxis of Metal–Phenolic Particle Microswimmers